Magmatic inclusions in martian meteorites

Yukio Ikeda

Department of Materials and Biological Sciences, Ibaraki University, Mito 310-8512
E-mail: y-ikeda@mx.ibaraki.ac.jp

Abstract: Magmatic inclusions in martian meteorites occur mainly within olivine and pyroxene grains. They are a few hundreds of micrometers to less than 10 micrometers across in size and have various mineral assemblages. They are grouped into five types on the basis of their silicate mineral assemblages, from glassy inclusions of type I to kaersutite-bearing inclusions of type V. The types of magmatic inclusions in shergottites reflect cooling rates of their host lithologies. The compositions of glasses in magmatic inclusions have a wide range, even if they occur within a single grain of olivine or pyroxene. The wide compositional range of the glasses in magmatic inclusions is caused by metastable crystallization of the residual melts; some magmatic inclusions crystallize only wall olivine, although some crystallize pyroxene, a silica mineral, plagioclase, or kaersutite in addition to wall olivine. The wide compositional range of glasses and the variety in texture and mineral assemblages of magmatic inclusions seem to be controlled by cooling rates of the host lithology, nucleation processes of the minerals, chemical compositions of the residual melts, and so on. The chemical trends of residual melts in magmatic inclusions are explained by using a pseudoternary phase diagram of quartz-olivine-plagioclase.

key words: martian meteorites, trapped melt, magmatic inclusions, metastable crystallization, glass

1. Introduction

Martian meteorites commonly contain magmatic inclusions, which occur in all SNC meteorite groups (shergottites, nakhlites, and. chassignite). They are included within olivine, pyroxene, chromite (or magnetite), and phosphate of the host lithologies, although those within olivine are predominant, and those within chromite and phosphate are rare. They are several to a few hundreds of μm in diameter, and rounded to subrounded in shape.

During crystallization of martian magmas, the liquid of magmas was trapped as melt inclusions within crystallizing host minerals, which resulted in magmatic inclusions. The melt inclusions experienced closed-system crystallization within the host minerals, except for exchange of Mg and Fe between the melt inclusions and the host mineral. In melt inclusions, the same mineral as the host phase easily grows without nucleation, lining the wall of the inclusions, and exceeding the amount expected from equilibrium crystallization. A new phase different from the host phase seems to be very

difficult to nucleate, resulting in metastable crystallization.   On the other hand, the crystallization of magmas for the host lithology shows an open-system and stable crystallization sequence.   Therefore, the metastable crystallization sequences for melt inclusions are quite different from the stable sequences for their host lithology.

As primary trapped liquid crystallizes first the "wall phase" surrounding the inclusions, the chemical compositions of the primary trapped liquid are mixtures of the compositions of magmatic inclusions themselves and a suitable amount of the wall phase.   Martian meteorites sometimes contain cumulus minerals, and the whole rock compositions do not necessarily represent the martian magmas.   Magmatic inclusions, however, give us direct information about the major element compositions of martian magmas in early to late stages of crystallization for the host lithology.

2.   Occurrence of magmatic inclusions

Many martian meteorites contain magmatic inclusions within olivine, pyroxenes, chromite, magnetite, and phosphate.   They are reported in many literatures and are summarized in Table 1.   Recently, new martian meteorites were recovered from hot deserts (Northwest Africa), but their detailed petrography is not yet reported.   Therefore, we do not know whether they contain magmatic inclusions or not, and most of NWA martian meteorites are listed in Table 1 with a symbol "?".

2.1.   Chassignite
The Chassigny meteorite contains magmatic inclusions within olivine, where kaersutite sometimes occurs in alkali-feldspar-rich glass (Floran *et al*., 1978).   According to Floran *et al*. (1978), the paragenetic sequence of crystallization for Chassigny melt inclusions is;

Wall olivine→pyroxene→kaersutite→chlorapatite

→ {pentlandite, chromite, troilite} →glass.

Johnson *et al*. (1991) reported occurrence of biotite in addition to kaersutite and two kinds of glasses in magmatic inclusions within olivine in Chassigny.   They concluded that the glasses appear to be "inclusion mesostasis" that was shock melted.   They also suggested from the occurrence of kaersutite that water ratio in the fluid in the Chassigny melt inclusions is estimated to have been at least 0.8 in order to stabilize kaersutite without plagioclase in a rhyolitic melt, implying that the water fugacity was ~1.48 kb.   However, Ti-oxy kaersutite seems to be stable at 1 bar pressure (Popp *et al*., 1995a, b), and the water fugacity of Chassigny melt inclusions can be far below 1.48 kb.   Varela *et al*. (2000) studied the glass inclusions within olivine in Chassigny and concluded that the inclusions were heterogeneously trapped in olivine and the glass is not residual melt but original trapped melt.

2.2.   Nakhlites
Nakhla and Governador Varadares contain magmatic inclusions (vitrophyric inclusions) within olivine (Harvey and McSween, 1992), and kaersutite was reported in some vitrophyric inclusions within olivine in Governador Varadares (Harvey and McSween,

Table 1. *Magmatic inclusions in martian meteorites. Open circles: magmatic inclusions occur within constituent minerals (mostly olivine; sometimes pyroxene, chromite, magnetite, and phosphate) of the host lithology. Question symbols: magmatic inclusions are not described in literatures.*

Group or Subgroup	Meteorites with order of date found, (1)–(32)	Magmat. Incl.
Chassignite Group	(1) Chassigny	○
Nakhlite Group	(3) Nakhla	○
	(4) Lafayette	○
	(5) Governador Varadares	○
	(20) Y000593, 749, 802	○
	(21) NWA817	○
	(25) NWA998 (Opx-bearing)	?
	(32) MIL03346	?
Orthopyroxenite Group	(10) ALH84001	no
Lherzolitic Shergottite Sugroup	(7) ALHA77005	○
	(8) Y-793605	○
	(11) LEW88516	○
	(17) GRV99027	?
	(27) YA1075 (not approved by MSNC)	?
	(30) NWA1950	?
Ol-phyric Shergottite Subgroup	(13) DaG476, 489, 670, 735, 876, 975	○
	(15) SaU005, 008, 051, 060, 090, 094, 125, 130	○
	(24) NWA1068, 1110	○
	(26) NWA1195 (Ol-Opx-phyric)	?
	(16) Dhofar 019 (Megacryst-poor)	○
	(9) EETA79001A (Xenolith-bearing)	○
	(28) Y980459 (Glassy type)	○
	(29) DaG1037	○
	(31) NWA2046 (Ol-Opx-phyric)	○
Basaltic Shergottite Subgroup	(2) Shergotty	○
	(6) Zagami	○
	(9) EETA79001B	○
	(12) QUE94201	?
	(14) Los Angeles	○
	(18) Dhofar 378	○
	(19) NWA480, 1460 (Gabbroic type)	?
	(22) NWA1669	?
	(23) NWA856	?

Ol: magnesian olivine, except fayalitic olivine.   Opx: orthopyroxene.
MSNC: Meteoritical Society Nomenclature Committee.

1991).   The vitrophyric inclusions in Nakhla and Governador Varadares consist mainly of augite and glass, and lack low-Ca pyroxene and plagioclase.   According to Harvey and McSween (1992), the reason for no low-Ca pyroxene in vitrophyric inclusions is that olivine was isolated from the Si-rich liquid by a protecting rind of augite, inhibiting crystallization of low-Ca pyroxene.   They explained the lack of plagioclase by an idea that H_2O contents increased in inclusions, resulting in inhibition of plagioclase crystallization.   Lafayette contains a diamond-shaped inclusion within olivine (Bunch and

Reid, 1975), which consists mainly of pyroxene and K-Si-rich glass.

Yamato-nakhlites (Y000593, Y000749, and Y000802) contain magmatic inclusions (vitrophyric inclusions) within olivine (Imae *et al*., 2004) similar to those in Nakhla. There are two types of vitrophyric inclusions, rounded and angular types. The rounded type represents a melt of early to middle stage crystallization of the parent magma, and the angular type represents the residual melts of the mesostasis stage of the host lithology (Imae *et al*., 2004). Small blebs, ~1 μm across, are abundant within pyroxene grains in Yamato-nakhlites, although the constituent phase (glass or fluid) in the small blebs is not identified (Imae *et al*., 2003). They may not be magmatic inclusions.

The NWA817 nakhlite contains magmatic inclusions within olivine (Sautter *et al*., 2002). The NWA 998 nakhlite contains trains of tiny glass blebs along healed fractures within pyroxenes (Russell *et al*., 2003). The tiny glass blebs consist mainly of K-Na-Al-bearing glass, and some of them occur as intergrowths of glass and Fe-bearing carbonate. They may not be magmatic inclusions, although it is not yet known whether true magmatic inclusions occur in NWA998 or not.

2.3. Lherzolitic shergottites

The ALH-77005 lherzolitic shergottite contains magmatic inclusions within olivine (Shih *et al*., 1982). Jagoutz (1989) found a silica mineral in magmatic inclusions within olivine in ALH-77005, and concluded that the apparent coexistence of a silica mineral within olivine was caused by metastable crystallization of a silica mineral in magmatic inclusions. Ikeda (1998) found that magmatic inclusions within olivine in ALH-77005 contain silica-rich glass and/or plagioclase-rich glass (or maskelynite) in addition to pyroxene, whereas magmatic inclusions within pyroxene contain kaersutite, but never contain silica-rich glass nor plagioclase-rich glass. Y-793605 contains magmatic inclusions within olivine and pyroxene (Ikeda, 1997), and they are very similar to those in ALH-77005, although kaersutite in Y-793605 seems to have decomposed into fine-rained aggregates by an intense shock.

LEW88516 contains magmatic inclusions within large olivine grains, and Harvey *et al*. (1993) found that there are two glasses, moderately Si-rich glass (SiO_2~65%) and extremely Si-rich glass (SiO_2>95%), suggesting liquid immiscibility in the melt inclusions.

2.4. Ol-phyric shergottites

DaG476 contains magmatic inclusions within olivine, which consist mainly of Al-Ti-rich pyroxene and feldspathic glass (Ziphel *et al*., 2000; Mikouchi *et al*., 2001). Folco *et al*. (2000) reported magmatic inclusions within olivine and chromite in DaG 489, and two types of glass in the inclusions. The two glasses are dacitic glass and Si-rich glass, which show a liquid immiscibility fabric in magmatic inclusions (Folco *et al*., 2000). DaG735 also contains magmatic inclusions within olivine (Ikeda, unpublished data), and the magmatic inclusions occur always within the olivine having the compositions of Fo_{60-62}, although phenocrystic olivine ranges in composition from Fo_{78} to Fo_{59}.

SaU 005 contains magmatic inclusions within olivine and chromite (Goodrich, 2003). The magmatic inclusions within olivine do not occur in olivine cores but in

olivine of Fo_{69-62}, and were grouped into two types, I and II; type I magmatic inclusions consist mainly of pyroxene and glass, whereas the type II consists mainly of pyroxene, Si-rich blebs, and Si-poor glass (Goodrich and Ziphel, 2001; Goodrich, 2003). Olivine in SaU005 ranges in composition from Fo_{71} to Fo_{60}, and the type I magmatic inclusions occur in olivine of Fo_{65-62}, whereas the type II occurs in more magnesian olivine of Fo_{70-65} (Ikeda, unpublished data).

NWA1068 contains magmatic inclusions within large olivine, and two immiscible SiO_2-rich glasses occur in inclusions (Barrat et al., 2002). There is no description of magmatic inclusions for NWA1195, but it may contain magmatic inclusions because the lithology is very similar to NWA2046 that contains magmatic inclusions (Irving et al., 2004). Dhofar 019 contains magmatic inclusions in olivine (Ikeda, unpublished data).

EETA79001 contains kaersutite in magmatic inclusions within pigeonite (Treiman, 1997). Treiman (1997) suggested that (1) melts of magmatic inclusions within pigeonite evolved toward depletion in SiO_2 and enrichment in CaO, Al_2O_3, and TiO_2 to produce kaersutite, (2) melts of magmatic inclusions within augite evolved toward depletion in CaO, and (3) melts of magmatic inclusions within olivine evolved toward enrichment in SiO_2. Goodrich (2003) reported magmatic inclusions within olivine and chromite in EETA79001 lithology A, and the magmatic inclusions within olivine always occur in the olivine having Fo_{76} to Fo_{60}. She found two glasses, Si-rich glass and Si-depleted glass in the magmatic inclusions. Berkley et al. (2000) reported the occurrence of pure Si-Al-rich glass blebs smaller than $10\,\mu m$ across within xenolithic orthopyroxene cores in EETA79001 lithology A, but the origin of the glass blebs is not clear.

Y980459 is a glassy shergottite consisting mainly of phenocrystic olivine and microphenocrystic pyroxene which set in glassy groundmass (Ikeda, 2004). Magmatic inclusions occur in olivine, and are mostly clean glass with or without minor crystallites. DaG 1037 also contains magmatic inclusions within megacrystic olivine (Russell et al., 2004). NWA2046 contains magmatic inclusions within olivine, in which an Mg-Al-Ca-Fe-bearing silicate (possibly amphibole ?) occurs (Irving et al., 2004).

2.5. Basaltic shergottites

Shergotty and Zagami shergottites contain magmatic inclusions within pigeonite, augite, magnetite, and whitlockite (Treiman, 1985; Lundberg et al., 1988; McCoy et al., 1992). Kaersutite occurs within pigeonite in the two meteorites (Treiman, 1985; Watson et al., 1994; Hale et al., 1999), and the mineral assemblages of the kaersutite-bearing inclusions are kaersutite+glass with minor amounts of spinel, magnetite, ilmenite, pyrrhotite, and/or whitlockite. Mixtures of maskelynite, alkali-feldspar glass, and silica glass in Shergotty magmatic inclusions were reported by Treiman (1985).

Pyroxenes in the QUE94201 shergottite contain no magmatic inclusions (Meyer, 2003), although it is not clear whether other phases such as phosphates in QUE94201 contain magmatic inclusions or not. Whitlockites in Los Angels (Rubin et al., 2000) and Dhofar 378 (Ikeda, in preparation) contain glass inclusions, which may represent their residual melts at the latest stage of their fractional crystallization.

3. Types of magmatic inclusions

Magmatic inclusions in martian meteorites are classified into five types, I, II, III, IV, and V on the basis of their silicate assemblages.   Type I inclusions consist mainly of glass which is free from any silicate minerals (Fig. 1a), although some contain small grains of non-silicate minerals such as sulfide, oxide (chromite, magnetite, ilmenite etc.), and phosphate.   Type II contains aluminous pyroxene (fassaite) and glass (Fig. 1b, c), and sometimes non-silicate minerals occur there.   Type III is similar to type II, but the former contains silica ovoids in glass (Fig. 1d).   The silica ovoids have oval shapes with several to a few tens of μm across and are directly set in dacitic to rhyolitic glass.   They may have originally been tridymite or cristobalite, but now they are glass.   Type IV contains vitrified plagioclase grains or plagioclase intergrowths in addition to pyroxene and silica ovoids (Fig. 1e).   The vitrified plagioclase was originally plagioclase, but it may have changed to plagioclase glass (or maskelynite) when the meteorite was ejected from Mars.   For brevity, I will call it ex-plagioclase.   The ex-plagioclase intergrowth is set in dacitic to rhyolitic glass and consists of intergrowth of ex-plagioclase, silica, and glass.   The intergrowth may have been originally formed as mixtures of plagioclase, a silica mineral, and minor interstitial mlet, although an intense shock may have changed them to glassy phases.   Type V contains kaersutite in magmatic inclusions within olivine in chassignite and nakhlites and within pigeonite in shergottites (Fig. 1f). Fine-grained aggregates occur in magmatic inclusions in pigeonite in ALH-77005 and Y-793605 lherzolitic shergottites, and the aggregates have a composition similar to kaersutite, suggesting that kaersutite in the meteorites may have been decomposed by the intense shock.   Generally, kaersutite-bearing inclusions do not contain silica ovoids, suggesting that kaersutite occurs in SiO_2-depleted melts in magmatic inclusions.

Occurrence of the five inclusion types among the various groups or subgroups of SNC meteorites is summarized in Table 2.   Magmatic inclusions in glassy shergottite (Y980459) are mainly type I, with minor type II containing crystallites (Fig. 1b). Magmatic inclusions in most olivine-phyric shergottites are type I to type III. Magmatic inclusions of basaltic and lherzolitic shergottites range from type II to type V.   There are no type IV inclusions in chassignite and nakhlites.

Y980459 shergottite has a glassy groundmass (Ikeda, 2004), indicating that it cooled rapidly on Mars surface.   The most olivine-phyric shergottites except Y980459 have doleritic textures with holocrystalline groundmass, and they cooled more slowly than the Y980459 and more rapidly than gabbroic rock with no groundmass.   Basaltic shergottites have doleritic textures with fine-grained groundmass or gabbroic texture with no groundmass, and they cooled moderately to slowly.   Lherzolitic shergottites have gabbroic textures, and they cooled slowly.   The nakhlites are cumulates that consist of cumulus phases and intercumulus mesostasis.   The intercumulus mesostasis consist mainly of plagioclase needles (or laths) and small pyroxene grains, suggesting that they cooled moderately.   Chassigny is also a cumulate, showing a dunitic texture, but its cooling rate is not clear.

The cooling rates of shergottites are shown in Table 2, where the inclusion types seem to correlate to the cooling rates of the host shergottites.   The types of magmatic inclusions in chassignite and nakhlites probably suggest that they could have cooled
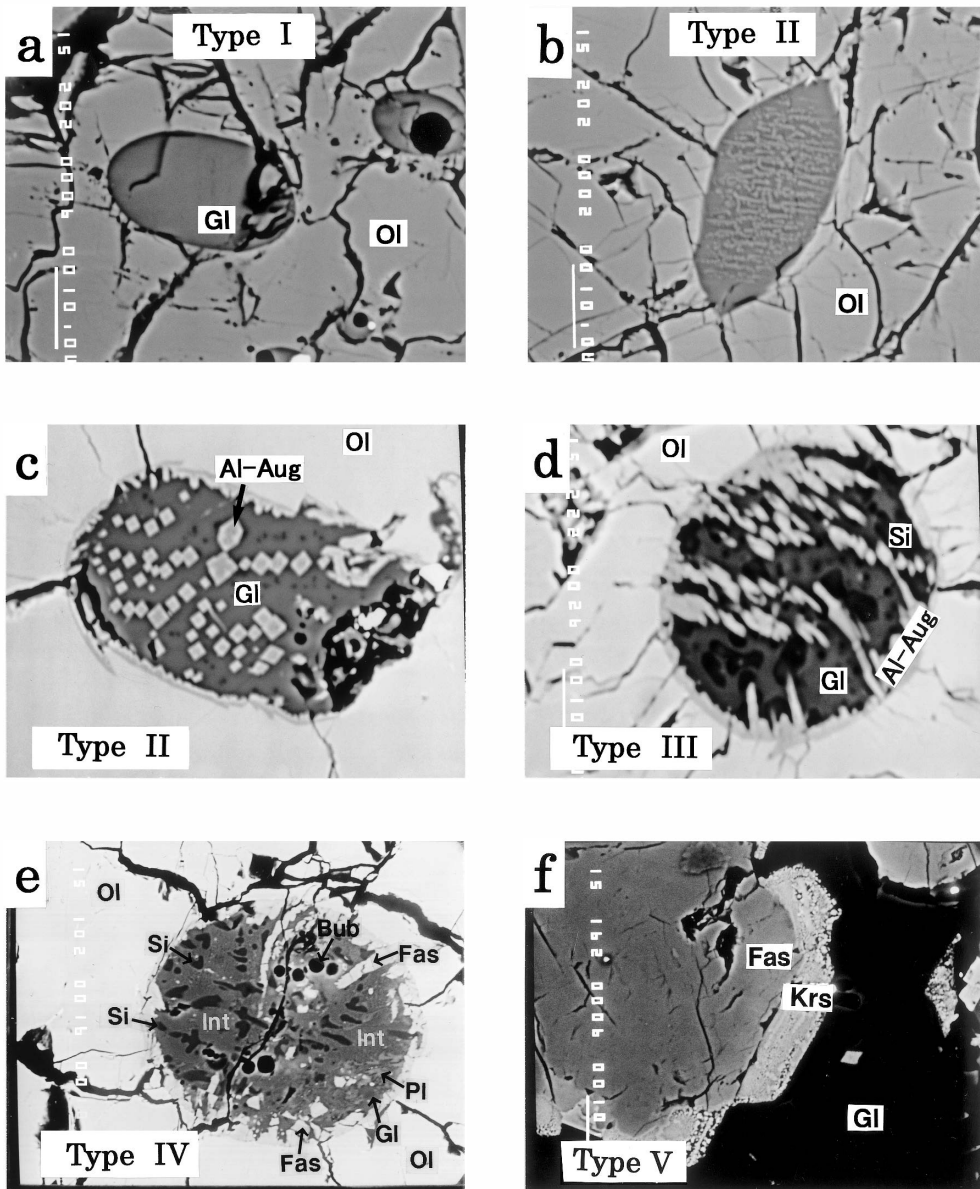
Fig. 1. *Back scattered electron (BSE) images of magmatic inclusions in martian meteorites.   (a) A glass (Gl) inclusion (type I) within olivine (Ol) in Y980459.   Width is 56 μm.   (b) A rare glassy inclusion including crystallites (type II) within olivine in Y980459.   Width is 56 μm.   (c) A type II inclusion consisting mainly of aluminous augite (Al-Aug) and glass (Gl) within olivine in SaU005.   Width is 70 μm.   (d) A type III inclusion consisting mainly of aluminous augite, silica ovoids (Si), and glass within olivine in SaU005.   Width is 51 μm.   (e) A type IV inclusion consisting mainly of fassaite (Fas), silica ovoids, ex-plagioclase (Pl), and intergrowth of ex-Pl, silica, and glass (Int) within olivine in ALH-77005.   Some bubbles (Bub) occur.   Width is 127 μm.   (f) Decomposition products of kaersutite (Krs) in a type V inclusion within pigeonite in ALH-77005.   Small kaersutite sometimes remains in the central portion of the fine-grained aggregates.   Width is 79 μm.*

Table 2. *Types of magmatic inclusions within olivine or pyroxene in martian meteorites. Type I (pure glass), type II (Pyroxene + Glass), type III (Silica ovoid-bearing), type IV (Ex-plagioclase-bearing) and type V (Kaersutite-bearing). The silica ovoid and ex-plagioclase were originally a silica mineral and plagioclase, but now they are silica-glass and plagioclase-glass (or maskelynite), respectively. Y98 is the Yamato 980459 glassy olivine(Ol)-phyric shergottite. Kaersutite (Krs) occurs in magmatic inclusions within olivine (Ol) or pigeonite (Pig).*

	Type I	Type II	Type III	Type IV	Type V	Cooling rate of host rocks
Glassy Ol-phyric Shergottite (Y98)	◯	◯				rapid
Non-glassy Ol-phyric Shergottites	◯	◯	◯			moderate
Basaltic Shergottites	(*1)	◯	◯	◯	◯ (Krs in Pig)	moderate~slow
Lherzolitic Shergottites		◯	◯	◯	◯ (Krs in Pig)	slow
Chassignite	◯(*2)	◯	◯		◯ (Krs in Ol)	
Nakhlites	(*3)	◯	◯		◯ (Krs in Ol)	

*1: Pure glass inclusions occur within whitlockite in Shergotty (Stolper and McSween, 1979; Lundberg *et al*., 1988), Zagami (Treiman, 1985), Los Angels (Rubin *et al*., 2000), and Dhofar 378 (Ikeda, in preparation).

*2: Pure glass inclusions, smaller than 10 μm across, within olivine in Chassigny was reported by Varela *et al*. (2000), but it is unclear whether they are truly magmatic inclusions or not.

*3: Trains of tiny glass blebs within pyroxene in the NWA998 nakhlite were reported (Russell *et al*., 2003), but they seem not to be magmatic inclusions. Fluid-like inclusions within augite occur in the Yamato 000593 nakhlite (Imae *et al*., 2003).

moderately. On the other hand, type V inclusions contains kaersutite, and crystallization of kaersutite is strongly controlled by the chemical compositions of residual melts in magmatic inclusions, as Treiman (1997) already suggested.

4. Crystallization of magmatic inclusions

Magmatic inclusions within olivine are the most common in martian meteorites, and crystallization of magmatic inclusions within olivine are schematically shown in Fig. 2. Magmatic inclusions within olivine phenocrysts in shergottites often occur in a narrow range of olivine, and they scarcely occur in the most magnesian cores and the most ferroan rims of olivine phenocrysts, suggesting that rapid growth of olivine took place in the middle stage of the olivine crystallization, which corresponds to early to middle stage of the whole rock crystallization.

(1) Rapid growth of olivine traps melts with or without minerals (Fig. 2). The originally trapped melt crystallizes wall olivine to line the inclusions. Generally, the crystallization of the wall olivine originally takes place in excess of equilibrium amounts under a metastable condition, and the residual melt extremely depleted in olivine components. The residual melt becomes enriched in silica and/or feldspar components (type I inclusions). The boundary between the host and wall olivines is unclear, because Mg-Fe diffusion takes place both between the two olivines and between the wall
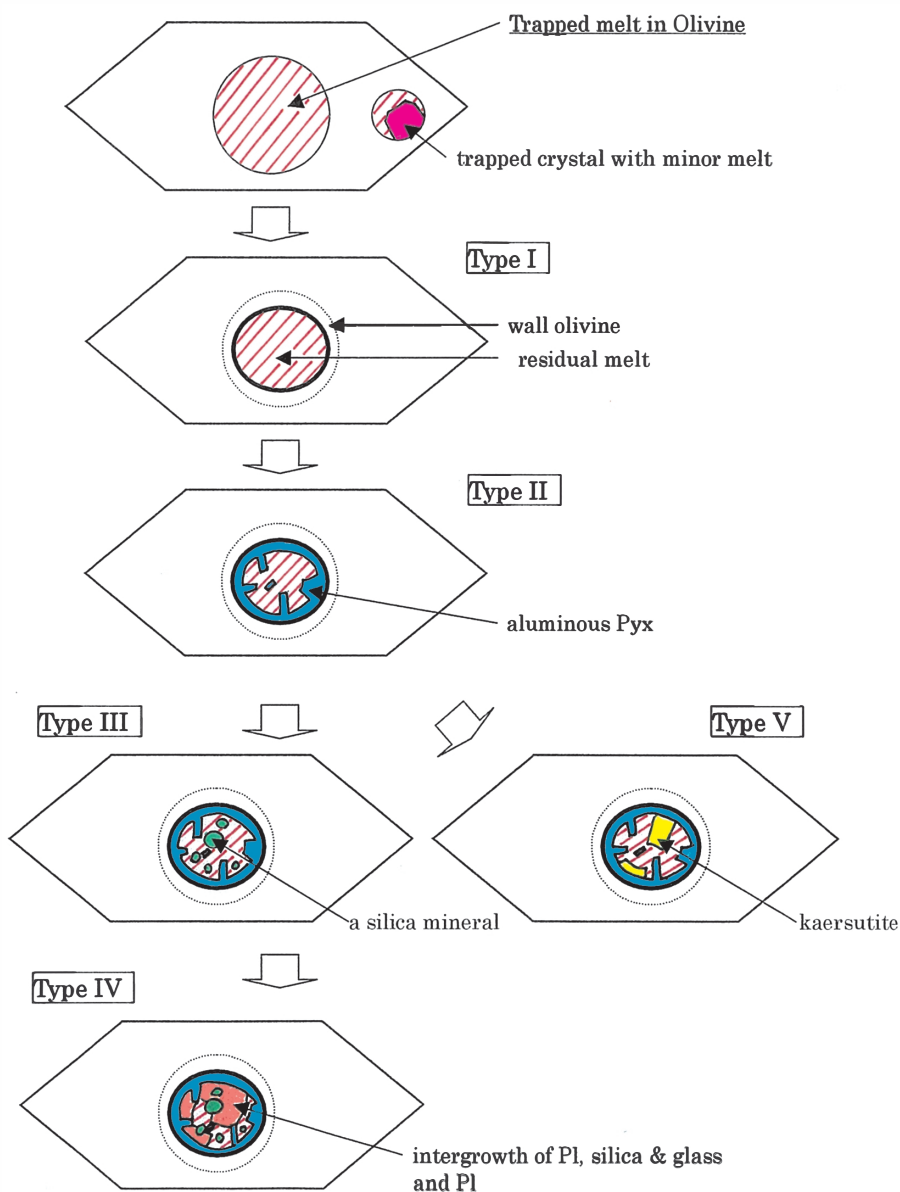
Fig. 2. *Types of magmatic inclusions within olivine in martian meteorites. A growing olivine grain traps silicate melts (red hatch), which sometimes associate crystals (pink) in inclusions. A trapped melt within olivine precipitates wall olivine lining the inclusion too much under a metastable condition, resulting in Si-Al-rich residual melt (type I). Aluminous pyroxene (blue) crystallizes from the residual melt, forming a mantle and/or floating grains in the inclusion (type II). A silica mineral grows in the Si-Al-rich residual melt that is already depleted in pyroxene components (type III). For the case that residual melts are Si-poor, kaersutite crystallizes, resulting in type V inclusions. Finally plagioclase crystallizes in the Si-Al-rich melt, and often it grows with a silica mineral and interstitial melt to form intergrowths of Pl, Si, and Gl (type IV).   Later, plagioclase and a silica mineral seem to have changed to plagioclase glass (or maskelynite) and silica glass, respectively, by an intense impact shock, and sometimes kaersutite decomposes into fine-grained aggregates by shock.*

olivine and the residual melt.   Therefore, usually we do not know the exact locality where the boundary between the host and wall olivine is.

(2)   Aluminous pyroxene (fassaite) crystallizes from the residual melt which is enriched in feldspar components, and type II inclusions are produced.   The Al_2O_3 contents of the aluminous pyroxene in type II inclusions are higher than those of the pyroxenes in the host lithology (Ikeda, 1998).   The aluminous pyroxene often forms a mantle surrounding the inclusions and grows needle crystals on the mantle or floating crystals in the inclusions (Fig. 2).

(3)   For the case that the residual melt is enriched in silica, a silica mineral (tridymite or cristobalite) crystallizes, and type III inclusions form.   For the case that the residual melt is not so enriched in silica, kaersutite crystallizes, resulting in type V inclusions.

(4)   After the crystallization of a silica mineral, the residual melt of type III inclusions becomes enriched in feldspar components, and precipitates plagioclase.   Usually the plagioclase grows together with a silica mineral, forming intergrowth of plagioclase and a silica mineral with minor interstitial melt (Ikeda, 1998).   Type IV inclusions are produced.

Magmatic inclusions belonging to a few types can occur within a single olivine grain: for example, type II inclusions coexist with type III inclusions within single olivine grains.   As the types II and III have similar compositions to each other, probably nucleation processes may control the crystallization of a silica mineral in the inclusion.

Martian meteorites suffered intense impact shock, which changed a silica mineral and plagioclase to silica melt (or glass) and plagioclase melt (glass or maskelynite), respectively.   Silica ovoids in type III may have originally been a silica mineral, but later an intense shock changed them to silica melt (or glass), which changed their outer shapes to ovals.   The silica melt (or glass) may have had high viscosity that prevented homogenization with ambient melts (or glasses).   The melts (or glasses) have quenched as silica glass under a rapid cooling condition after the excavation from Mars.   Ex-plagioclase in type IV inclusions is now plagioclase glass (or maskelynite), and it originally formed as plagioclase grains in the same way as silica ovoids.

The trapped melt crystallizes wall olivine and inclusion minerals in magmatic inclusions, and the melt fractionates to residual melts.   Finally the residual melts quench under various cooling conditions as glasses having various compositions.   The chemical compositions of residual-melt glasses in types I to V are shown in Table 3.

5.   Chemical compositions of original trapped liquids in olivine grains

Chemical compositions of magmatic inclusions are obtained as a mixture of the constituent minerals and glass.   Those for types I, II or III are glass, a mixture of glass and pyroxene, or a mixture of glass, pyroxene, and silica ovoids, respectively.   However, it is very difficult to obtain the correct modal compositions of the constituent phases, because the cut surface on a thin section is not necessarily representative.   The compositions of type I inclusions are the most accurate because the ambiguity of modal abundance is not introduced in the chemical compositions of the inclusions.

Table 3. *Chemical compositions of glasses in magmatic inclusions from shergottites.*
Olivine (Ol), glass (Gl), whitlockite (Wtl), and pyroxene (Pyx).

| | Glassy Ol-phyric | Non-glassy Ol-phyric | | | Basaltic | Lherzolitic | | | |
| | Y980459 | DaG735 | | | Dhofar378 | ALH-77005 | | | |
	Type I within Ol	Type I	Type II within Ol	Type III	Type I within Wtl	TypeII within Ol	TypeIII	TypeIV	TypeV within Pyx
SiO_2	62.15	60.77	65.02	66.10	69.63	65.21	61.28	72.94	65.28
TiO_2	0.92	1.02	1.22	0.32	0.38	0.40	0.32	0.68	0.27
Al_2O_3	11.49	15.43	15.19	20.55	12.90	19.16	21.23	16.42	19.49
Cr_2O_3	0.14	0.00	0.02	0.00	0.00	0.00	0.00	0.00	0.00
FeO	6.68	3.27	2.73	2.42	7.05	1.50	1.98	0.68	1.01
MnO	0.19	0.00	0.06	0.25	0.00	0.00	0.17	0.00	0.15
MgO	2.47	0.90	1.75	0.68	0.05	0.35	0.48	0.24	0.25
CaO	13.18	14.58	9.13	5.23	3.98	3.36	6.40	3.35	2.47
Na_2O	1.34	2.11	3.27	4.63	2.74	5.78	4.38	3.28	5.51
K_2O	0.06	0.10	0.12	0.08	3.02	1.76	1.75	2.04	4.66
P_2O_5	0.58					0.71	0.67	0.39	0.42
Total	99.18	98.18	98.53	99.75	99.75	98.23	98.66	100.02	99.51

Data sources: Y980459 (Ikeda, 2004), DaG735 and Dhofar378 (Ikeda, unpublished data), ALH-77005 (Ikeda, 1998).

The apparent trapped melts within olivine can be estimated from the chemical composition of magmatic inclusions by addition of wall olivine surrounding the inclusions;

Apparent trapped melt (L_T') = Magmatic inclusions + Wall olivine.

The wall olivine is added until the melt composition comes to a liquid which crystallizes olivine stably—This is a requirement for the original magma trapped in the olivine. The stable crystallization of olivine takes place within an olivine liquidus field of phase diagrams. However, there is a problem that the exact amount to be added is not known, because the wall olivine has nearly the same compositions as the surrounding host olivine and there is no boundary between the host and wall olivines. Therefore, it may be a safe rule that the apparent trapped melt is taken to be just on the liquidus field boundary between olivine and pyroxene so that we can obtain the amount of wall olivine to estimate the apparent compositions using a suitable phase diagram. Finally we should correct the mg ratios of the apparent trapped melts using partition coefficients between olivine and melts, because the compositions of the original trapped melts should be in equilibrium with the host olivine.

Magmatic inclusions within olivine in nakhlites were used for the estimation of the parental magma of nakhlites, and Harvey and McSween (1992) obtained the NIM (nakhlite inclusion median) composition for the parent magma of the nakhlites. The trapped melt compositions within olivine in the chassignite was estimated by Floran *et al*. (1978) and Johnson *et al*. (1991). The magmatic inclusions in the ALH-77005 lherzolitic shergottite were also used for estimation of the trapped melts within olivine

(Ikeda, 1998).

6. Crystallization trends of magmatic inclusions

Original trapped melts within olivine in shergottites crystallize wall olivine and then constituent minerals, resulting in types I, II, III and IV inclusions. A few types can occur within a single olivine grain, suggesting that nucleation of pyroxene, a silica mineral, or plagioclase is a delicate controlling factor during the crystallization.

Melt trends for shergottites and nakhlites (Ikeda, 2005) are shown in Fig. 3, where major crystallization trends for magmatic inclusions in martian meteorites are schematically shown. There are four major trends, α, β, γ, and δ. Trend α indicates that an early-stage magma is trapped within growing olivine and it changes by subtraction of wall olivine to a residual melt having an olivine-depleted and Si-enriched
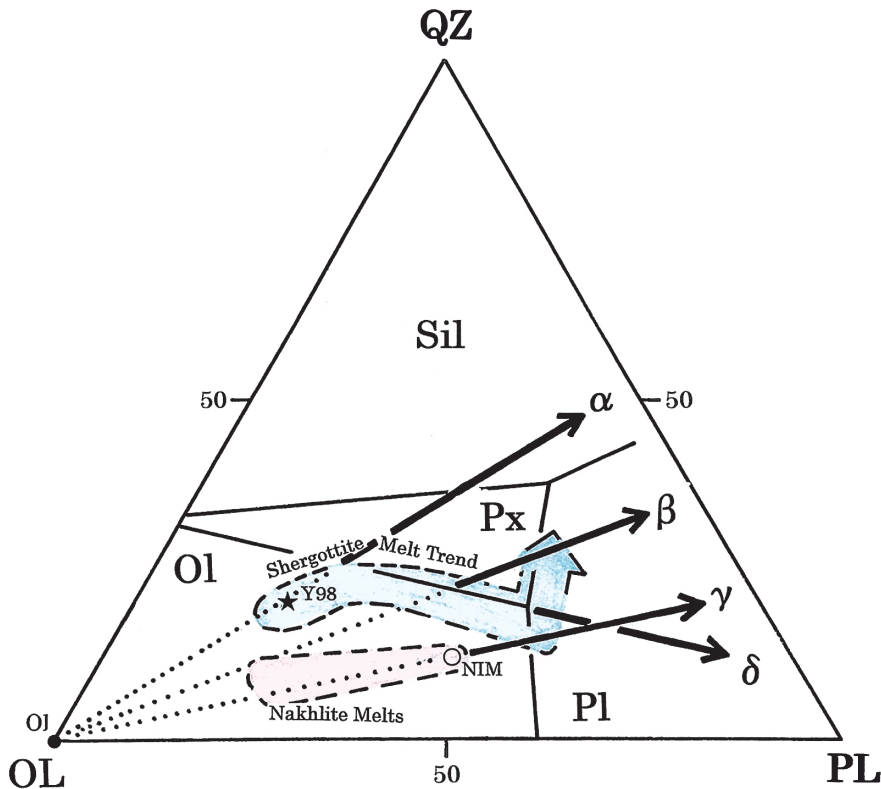
Fig. 3. *Major compositional trends (α, β, γ, δ) of magmatic inclusions are shown in the pseudoternary system of quartz(QZ)–olivine(OL)–plagioclase(PL) with mg=0.562 and An=77 (Longhi and Pan, 1989; Oxygen units projected from Wo) (see text). Primary liquidus fields of a silica mineral (Sil), low-Ca pyroxene (Px), olivine (Ol), and plagioclase (Pl) are shown together with the liquidus field boundaries between them (bold lines). Shergottite melt trend (blue range) and nakhlite melts (pink range) are quoted from (Ikeda, 2005) with the bulk composition of Y980459 (Y98, closed star) and nakhlite inclusion median (NIM, open circle; Harvey and McSween, 1992).*

composition.   This trend can produce magmatic inclusions of types I, II, III and/or IV.
Trend β indicates that a middle-stage magma is trapped within olivine and it changes to
a residual melt having an olivine-depleted and moderately Si-enriched composition.
This trend can produce inclusions of types I, II, III, and/or IV.   Trend γ indicates that
Si-poor magma is trapped within olivine, and the residual melt becomes enriched in
feldspar components.   This trend can produce inclusions of types I, II, and/or V.
Trend δ indicates that a magma is trapped within low-Ca pyroxene, and the residual
melt become enriched in feldspar components.   This trend can produce inclusions of
types I, II, and/or V.

Magmatic inclusions within olivine in nakhlites and chassignite take the trend γ,
and sometimes kaersutite occurs there, although inclusions within pigeonite in
shergottites take trend δ, and kaersutite also occurs there.   However, kaersutite never
occur in trends α and β, but silica ovoids occur there instead of kaersutite.   Kaersutite
in type V inclusions may be more easily produced under high water fugacity in their
inclusions.

7.   Crystallization trends for magmatic inclusions in DaG 735

One example for estimation of trapped melts within olivine in the DaG 735
olivine-phyric shergottite is shown in Table 4.   Wall olivine surrounding type I inclu-
sions is shown there, and the composition of the apparent trapped inclusion (L_T' in Table
4) was calculated from the wall olivine and the coexisting type I glass shown in Table
3.   The amount of wall olivine to be added was determined using the pseudoternary

Table 4.   *Chemical compositions of wall olivine around inclusions, fassaite in inclusions, apparent trapped*
melt within olivine (L_T'), and original trapped melt (L_T) in DaG 735.   The apparent trapped melt
(L_T') is obtained from an equation [(type I glass) $\times 2$ + (Wall olivine) $\times 1$] (see text).   The type I
glass is shown in Table 3.   The original trapped melt (L_T) is estimated from the apparent melt (L_T'),
using an Mg-Fe partition coefficient between olivine and melt ($K = 0.35$; Stolper, 1977) in order to
be in equilibrium with the wall olivine (Fo_{61}).   Chemical compositions of the groundmass (Gdm)
in DaG 476 (Zipfel et al., 2000), aluminous pyroxene (Fas) in inclusions within olivine in DaG735,
and Shergotty intercumulus liquid (SILC; Hale et al., 1999) are shown for reference.

	DaG735 Wall Ol	DaG735 L_T'	DaG735 L_T	DaG476 Gdm	DaG735 Fas	Shergotty SILC
SiO_2	36.44	53.37	51.74	50.95	44.97	50.8
TiO_2	0.01	0.70	0.68	0.51	3.15	1.0
Al_2O_3	0.02	10.43	10.11	5.66	9.02	8.0
Cr_2O_3	0.00	0.00	0.00	0.92	0.05	-
FeO	33.27	13.45	20.04	15.46	11.44	19.8
MnO	0.62	0.21	0.20	0.47	0.30	0.5
MgO	28.98	10.40	6.15	18.32	8.38	7.7
CaO	0.22	9.93	9.62	7.04	21.31	9.7
Na_2O	0.04	1.44	1.40	0.67	0.33	1.5
K_2O	0.01	0.07	0.06	-	0.02	0.2
P_2O_5	-	-	-	-	-	0.9
Total	99.61	100.00	100.00	100.00	98.96	100.1
mg	0.61	0.58	0.35	0.68	0.57	0.42
norm An	-	62	62	67.4	-	50

phase diagram of Quartz-Olivine-Plagioclase (Fig. 3, mg＝0.562, An＝77; Longhi and Pan, 1989) so that the trapped melt is just on the liquidus phase boundary between olivine and low-Ca pyroxene fields.   The resulting ratio of the glass (Table 3, type I) to the wall olivine (Table 4) is 2:1.   The original trapped melt (L_T in Table 4) is estimated by correction of the apparent melt composition (L_T' in Table 4) using the Mg-Fe partition coefficient between olivine (mg＝0.61) and melt (K＝0.35; Stolper, 1977).   This calculation changes the mg of 0.58 for the apparent trapped melt inclusion to 0.35 for the original trapped melt (Table 4).   The calculated original trapped melt is more evolved than the chemical composition of the groundmass in DaG 476 (paired with DaG735) obtained by Ziphel $et\ al.$ (2000), and it is very similar to the Shergotty intercumulus liquid composition (SILC in Table 4).   As already stated in section 2–4, magmatic inclusions in DaG 735 occur within the olivine of $Fo_{60–62}$, suggesting that the trapped melts represent the magma of the middle stage, and the crystallization of the inclusions may take the major trend β in Fig. 3.

　　The glasses in magmatic inclusions within olivine in DaG 735 are plotted in Fig. 4, where the chemical compositions of wall olivine, fassaite and silica ovoids in magmatic inclusions of DaG735 are shown.   The representative compositions of wall olivine and fassaite in inclusions are tabulated in Table 4.   The original trapped melt (L_T in Table 4) is shown by an open star in Fig. 4, and three sub-trends are shown by two open arrows and one closed arrow.   Trend β_1 produces type I inclusions, by subtraction of wall olivine from the original trapped melt.   After precipitation of wall olivine, fassaitic
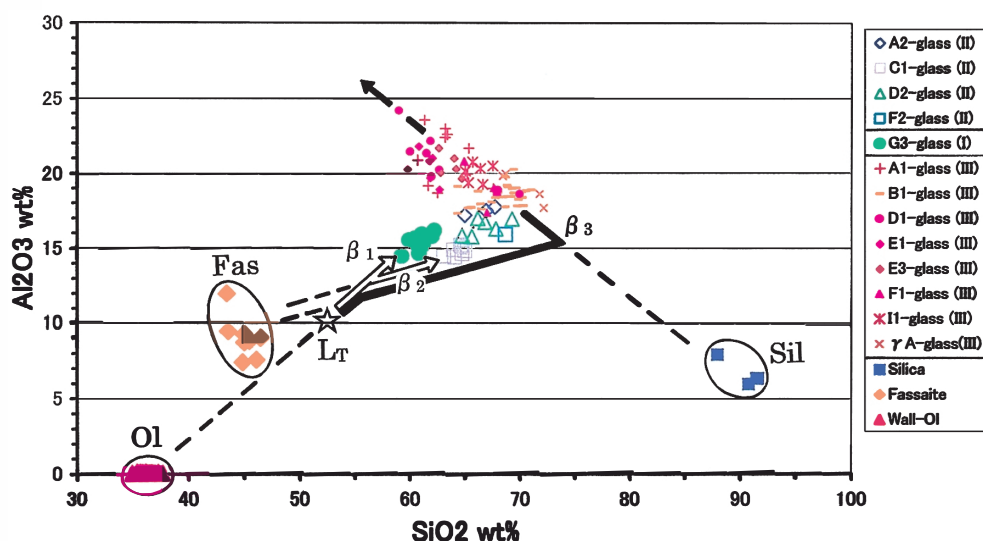
Fig. 4.   Glasses in magmatic inclusions (types I, II, III) within olivine in DaG 735.   Wall olivine (Ol), aluminous pyroxene (Fas), and silica ovoids (Si) in inclusions are shown for reference.   Major trend β in Fig. 3 splits into three sub-trends, β_1, β_2, β_3.   Type I glass inclusions form by sub-trend β_1 through precipitation of wall olivine, crystallization of aluminous pyroxene makes type II inclusions by β_2, and type III inclusions form through precipitation of a silica mineral (Si), with residual melt of sub-trend β_3 (see text).

pyroxene crystallizes in inclusions, and trend β_2 produces type II inclusions by subtraction of the fassaitic pyroxene. After precipitation of wall olivine and fassaitic pyroxene, a silica mineral crystallizes from Si-enriched residual melts to form trend β_3, resulting in type III inclusions.

The three sub-trends are shown in the pseudoternary phase diagram of Quartz-Olivine-Plagioclase (Fig. 5). The parental magma for the main lithology of DaG 735 may have a composition similar to that of the DaG 476 groundmass ($L_{G_{dm}}$ in Fig. 5) obtained by Ziphel et al. (2000), and the magma may evolve toward the invariant point between olivine, pyroxene, and plagioclase liquidus fields which is indicated by a hatched arrow in Fig. 5. A middle-stage magma (L_T) was trapped within olivine, and because pyroxene failed to nucleate it evolved toward olivine-depleted residual melts, which are

Fig. 5. *Representative glasses in magmatic inclusions within olivine in the DaG 735 olivine-phyric*
shergottite are plotted in the pseudoternary system of Quartz–Olivine–Plagioclase in oxygen units
projected from Wo (Longhi and Pan, 1989). Open circles (glasses in types I and II inclusions),
closed circles (glasses in types III). A hatched arrow is the crystallization trend for the host
lithology of DaG 735, and the mg ratios of DaG 735 magma change from 0.68 of the groundmass
(L_{Gdm} in Table 4; Ziphel et al., 2000) to less than 0.35 (L_T in Table 4). SILC is the shergotty
interstitial liquid composition obtained by Hale et al. (1999), and L_T is the trapped melt within
olivine in DaG 735. Olivine, plagioclase, low-Ca pyroxene (Px), fassaite (Fas, Table 4), and a
silica mineral are shown by solid stars. Major trend β (Fig. 3) of residual melts in melt
inclusions is shown by open arrows (β_1 and β_2) and a solid arrow (β_3). The dashed lines mean
the subtraction of olivine or fassaite from the residual melts.

quite different from the main magmatic trend for the host lithology. After precipitation of wall olivine, pyroxene crystallizes from Si-Al-Ca-Ti-rich residual melts, and the pyroxene is extremely enriched in Al, resulting in fassaitic pyroxene in inclusions. The fassaite (Table 4) differs in composition from the pyroxene of the host lithology, and plots within the olivine liquidus field, as shown in Fig. 5. Trend β_3 goes toward Si-rich residue by crystallization of fassaite earlier than trend β_2. This trend crystallizes a silica mineral (probably tridymite or cristobalite), and the residual melts turn toward feldspar-rich residues (Fig. 5).

8. Summary

The example of DaG 735 suggests that major trend β in Fig. 3 splits into three sub-trends of $\beta_1, \beta_2,$ and β_3, resulting in types I, II, and III inclusions. The other major trends, $\alpha, \gamma,$ and δ may also have sub-trends similar to those of trend β. The magmatic inclusions in martian meteorites show diversification in texture and mineral assemblage, and this diversity may be explained by the above-stated scenario containing the sub-trends.

Mineral assemblages of magmatic inclusions seem to be controlled by (A) cooling rate of the host lithology, (B) chemical compositions of melts in inclusions, (C) nucleation of minerals in inclusions, (D) fugacities of H_2O or O_2 in inclusions. Magmatic inclusions in shergottites may be intensely controlled by (A) cooling rates of the host lithology, as shown in Table 2. Silica ovoids never coexist with kaersutite in magmatic inclusions, suggesting that crystallization of a silica mineral or kaersutite may be affected by (B) the chemical composition. Several types of magmatic inclusions commonly occur within single olivine grains, although they have chemical compositions similar to each other, suggesting that they are controlled by (C) delicate nucleation processes. The delicate nucleation processes may be affected by such factors as surface energy between inclusion melts and the host mineral, existence of embryos in magmatic inclusions, dispersion efficiency of latent heat due to crystallization of minerals, and so on. Crystallization of some minerals such as spinel or magnetite may be controlled by (D) fugacity of O_2, and occurrence of kaersutite by (D) fugacities of H_2O and O_2.

References

Barrat, J.A., Jambon, A., Bohn, M., Gillet, PH., Sautter, V., Goepel, C., Lesourd, M. and Keller, F. (2002): Petrology and chemistry of the picritic shergottite North West Africa 1068 (NWA 1068). Geochim. Cosmochim. Acta, **66**, 3505–3518.

Berkley, J.L., Treiman, A.H. and Jones, J.H. (2000): Petrologic history of a complex pyroxenite xenolith in the EETA79001 martian meteorite. Lunar and Planetary Science XXXI. Houston, Lunar Planet. Inst., Abstract #1729 (CD-ROM).

Bunch, T.E. and Reid, A.M. (1975): The nakhlites Part I: Petrography and mineral chemistry. Meteoritics,

10, 303–324

Folco, L., Franchi, I.A., D'Orazio, M., Rocchi, S. and Schultz, L. (2000): A new martian meteorite from the Sahara: The shergottite Dar al Gani 489. Meteorit. Planet. Sci., **35**, 827–839.

Floran, R.J., Prinz, M., Hlava, P.F., Keil, K., Neil, C.E. and Hinthorne, J.R. (1978): The Chassigny meteorite: a cumulate dunite with hydrous amphibole-bearing inclusions. Geochim. Cosmochim. Acta, **42**, 1213–1239.

Goodrich, C.A. (2003): Petrogenesis of olivine-phyric shergottites Sayh al Uhaymir 005 and Elephant Moraine A79001 lithology A. Geochim. Cosmochim. Acta, **67**, 3735–3772.

Goodrich, C.A. and Ziphel, J. (2001): Magmatic inclusions in olivine and chromite in basaltic shergottite Sayh al Uhaymir 004: implications for petrogenesis and relationships to lherzolitic shergottites. Lunar and Planetary Science XXXII. Houston, Lunar Planet. Inst., Abstract #1174 (CD-ROM).

Hale V.P., McSween, H.Y. and McKay, G.A. (1999): Re-evaluation of intercumulus liquid composition and oxidation state for the -Shergotty meteorite. Geochim. Cosmochim. Acta, **63**, 1459–1470.

Harvey, R.P. and McSween, H.Y. (1991): Parental magmas of the nakhlites: Clues from the mineralogy of magmatic inclusions. Meteoritics, **26**, 343.

Harvey R.P. and McSween H.Y. (1992): The parent magma of the nakhlite meteorites: Clues from melt inclusions. Earth Planet. Sci. Lett., **111**, 467–482.

Harvey R.P., Wadhwa, M., McSween, H.Y. and Crozaz, G. (1993): Petrography, mineral chemistry, and petrogenesis of Antarctic shergottite LEW88516. Geochim. Cosmochim. Acta, **57**, 4769–4783.

Ikeda, Y. (1997): Petrology and mineralogy of the Y-793605 martian meteorite. Antarct. Meteorite Res., **10**, 13–40

Ikeda, Y. (1998): Petrology of magmatic silicate inclusions in the Allan Hills 77005 lherzolitic shergottite. Meteorit. Planet. Sci., **33**, 803–812.

Ikeda, Y. (2004): Petrology of the Y980459 shergottite. Antarct. Meteorite Res., **17**, 35–54.

Ikeda, Y. (2005): Unusual inclusions within olivine megacrysts in the Daral Gani 735 shergottite. Antarct. Meteorite Res., **18**, 202–212.

Imae, N., Ikeda, Y., Shinoda, K., Kojima, H. and Iwata, N. (2003): Yamato nakhlites: Petrography and mineralogy. Antarct. Meteorite Res., **16**, 13–33.

Imae, N., Ikeda, Y. and Kojima, H. (2004): Petrology of the Yamato nakhlites. submitted to Meteorit. Planet. Sci.

Irving, A.J., Bunch, T.E., Kuehner, S.M and Wittke, J.H. (2004): Petrology of primitive olivine-orthopyroxene-phyric shergottites NWA2046 and NWA1195: Analogies with terrestrial boninites and implications for partial melting of hydrous martian mantle. Lunar and Planetary Science XXXV. Houston, Lunar Planet. Inst., Abstract #1444 (CD-ROM).

Jagoutz, E. (1989): Sr and Nd isotopic systematics in ALHA77005: Age for shock metamorphism in shergottites and magmatic differentiation on Mars. Geochim. Cosmochim. Acta, **53**, 2429–2441.

Johnson, M.C., Rutherford, M.J. and Hess, P.C. (1991): Chassigny petrogenesis: Melt compositions, intensive parameters, and water contents of Martian (?) magmas. Geochim. Cosmochim. Acta, **53**, 349–366.

Longhi, J. and Pan, V. (1989): The parent magmas of the SNC meteorites. Proc. Lunar Planet. Sci. Conf., **19th**, 451–464.

Lundberg, L.L., Crozaz, G., McKay, G. and Zinner, E. (1988): Rare earth element carriers in the shergotty meteorite and implications for its chronology. Geochim. Cosmochim. Acta, **52**, 2147–2163.

McCoy, T.J., Taylor, G.F. and Keil, K. (1992): Zagami: Product of a two-stage magmatic history. Geochim. Cosmochim. Acta, **56**, 3571–3582.

Meteorite Working Group (2004): Antarctic Meteorite Newsletter-2004 July. **27** (2).

Meyer, C. (2003): Mars Meteorite Compendium-2003. XII. QUE94201, XII-1 to XII-9. Houston, Johnson Space Center.

Mikouchi, T., Miyamoto, M. and McKay, G.A. (2001): Mineralogy and petrology of the Dar al Gani 476 martian meteorite: Implications for its cooling history and relationship to other shergottites. Meteorit. Planet. Sci., **36**, 531–548.

Popp, R.K., Virgo, D., Yoder, H.S., Jr., Hoering, T.C. and Phillips, M.W. (1995a): An experimental study of phase equilibria and Fe oxy-component in kaersutitic amphibole: Implications for the f_{H_2} and a_{H_2O} in the upper mantle. Am. Mineral., **80**, 534–548.

Popp, R.K., Virgo, D. and Phillips, M.W. (1995b): H deficiency in kaersutitic amphiboles: Experimental verification. Am. Mineral., **80**, 1347–1350.

Rubin, A.E., Warren, P.H., Greenwood, J.P., Verish, R., Leshin, L.A. and Hervig, R.L. (2000): Petrology of Los Angels: A new basaltic shergottite find. Lunar and Planetary Science XXXI. Houston, Lunar Planet. Inst., Abstract #1963 (CD-ROM).

Russell, S.S., Zipfel, J., Folco, L., Jones, R., Grady, M.M., McCoy, T.M. and Grossman, J.N. (2003): The Meteoritical Bulletin No. 87, 2003 July. Meteorit. Planet. Sci., **38** (Suppl.), A203.

Russell, S.S., Folco, L., Grady, M.M., Zolensky, M.E., Jones, R., Richter, K., Zipfel, J. and Grossman, J.N. (2004): The Meteoritical Bulletin No. 88, 2004 July. Meteorit. Planet. Sci., **39** (Suppl.), A217.

Sautter, V., Barrat, J.A., Jambon, A., Lorand, J.P., Gillet, P., Javoy, M., Joron, J.L. and Lesourd, M. (2002): A new martian meteorite from Morocco: The nakhlite North West Africa 817. Earth Planet. Sci. Lett., **195**, 223–238.

Shih, C.Y., Nyquist, L.E., Bogard, D.D., McKay, G.A., Wooden, J.L., Bansal, B.M. and Wiesmann, H. (1982): Chronology and petrogenesis of young achondrites, Shergotty, Zagami, and ALHA77005: Late magmatism on a geological active planet. Geochim. Cosmochim. Acta, **46**, 2323–2344.

Stolper, E.M. (1977): Experimental petrology of eucritic meteorites. Geochim. Cosmochim. Acta, **41**, 587–611.

Treiman, A.H. (1985): Amphibole and hercynite spinel in shergotty and Zagami: Magmatic water, depth of crystallization, and metasomatism. Meteoritics, **20**, 227–242.

Treiman, A. (1997): Amphibole in martian meteorite Elephant Moraine 79001. Meteorit. Planet. Sci., **32** (Suppl), A129–A130.

Varela, M.E., Kurat, G., Bonnin-Mosbah, M., Clocchiatti, R. and Massare, D. (2000): Glass-bearing inclusions in olivine of the Chassigny achondrite: Heterogeneous trapping at sub-igneous temperatures. Meteorit. Planet. Sci., **35**, 39–52.

Watson, L.L., Hutcheon, I.D., Epstein, S. and Stolper, E.M. (1994): Water on Mars: Clues from deuterium/hydrogen and water contents of hydrous phases in SNC meteorites. Science, **265**, 86–90.

Zipfel, J., Scherer, P., Spettel, B., Dreibus, G. and Schultz, L. (2000): Petrology and chemistry of the new shergottite Dar al Gani 476. Meteorit. Planet. Sci., **35**, 95–106.